5th International Conference on
Structural Health Monitoring of Intelligent Infrastructure (SHMII-5) 2011
11-15 December 2011, Cancún, México

MONITORING OF A NOVEL FLEXIARCH™ BRIDGE SYSTEM TO INVESTIGATE SOIL-STRUCTURE INTERACTION

M. Lydon, S.E. Taylor, V. Sivakumar (DSc), D Robinson and D. Hughes

School of Planning, Architecture and Civil Engineering, Queen's University Belfast, NI

ABSTRACT: Masonry arch bridges are one of the oldest forms of bridge construction and have been around for thousands of years. Brick and stone arch bridges have proven to be highly durable as most of them have remained serviceable after hundreds of years. In contrast, many bridges built of modern materials have required extensive repair and strengthening after being in service for a relatively short part of their design life. This paper describes the structural monitoring of a novel flexible concrete arch known as: FlexiArch™. This is a bridge system that can be transported as a flat-pack system to form an arch in-situ by the use of a flexible polymeric membrane. The system has been developed under a Knowledge Transfer Partnership between Queen's University Belfast (QUB) and Macrete Ltd. Tievenameena Bridge in Northern Ireland was a replacement bridge for the Northern Ireland Roads Service and was monitored under different axle loadings using a range of sensors including discrete fiber optic Bragg gratings to measure the change in strain in the arch ring under live loading. This paper discusses the results of a laboratory model study carried out at QUB. A scaled arch system was loaded with a simulated moving axle. Various techniques were used to monitor the arch under the moving axle load with particular emphasis on the interaction of the arch ring and engineered backfill.

1 INTRODUCTION

Bridge construction and maintenance contributes greatly to the environmental impact of our infrastructure. Masonry arch bridges are of particular interest, as increasing life cycle costs caused by high maintenance requirement of traditional bridges have made FlexiArch as a viable option. The FlexiArch is a novel system which offers a more environmentally friendly alternative to traditional arch bridges. The system consists of a number of unreinforced pre-cast concrete voussoirs which are connected together with a polymeric grid (Figure 1). This is new system and there is limited knowledge on how the FlexiArch interacts with the backfill material, particularly in relation to the lateral reaction of the abutments. This paper reports the observations made on a model FlexiArch system tested at QUB under various loading conditions. The model was instrumented with structural health monitors (SHM) in order to evaluate and understand the interaction between the FlexiArch and the backfill material. The response of the structure to the applied moving traffic load was monitored and recorded. The SHM has also validated non-linear finite element analysis (NLFEA) of the system particularly in respect to soil-structure interaction.

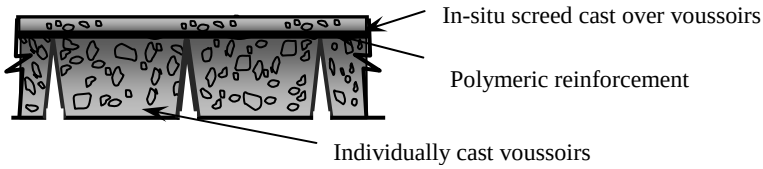

Figure 1: Construction of arch unit using pre-cast individual voussoir concrete blocks.

2 ARCH PROFILE AND MONITORING

2.1 Arch system detail

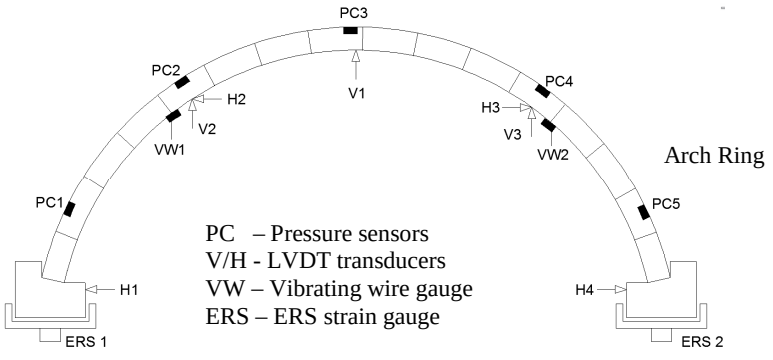

Arch Ring

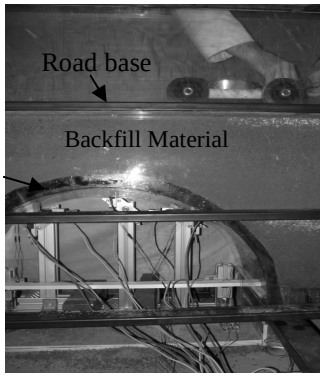

Figure 2: Typical arrangement of instruments and General set up.

A one sixth scale of a 5m span by 2m rise arch ring was used for this study. The arch was constructed based on the configuration reported by Taylor et al. (2008). The arch ring was monitored during the backfilling process. The abutments were supported horizontally with a spring on each side to represent weaker soil or not fully compacted backfill at the abutments. This was done to examine how lateral movement would affect the behavior of the arch bridge system.

2.2 Instrumentation and monitoring

The behavior of the structure was examined, particularly with respect to the arch/backfill interaction; to do this a range of sensors were used. The typical arrangement and loading is shown in Figure 2. Pressure cells were installed into five of the voussoirs. Seven LVDT (Linear Variable Differential Transformer) were used to measure the deflection of the arch ring. As the direction of movement is two dimensional, vertical and horizontal LVDT(s) were used to capture the resultant deformation. The opening between the voussoirs was measured using vibrating wire strain gauges (VWG). The arch was supported on rigid steel beams (as shown in Figure 2b) and it was gauged with ERS sensors to determine the vertical reactions at the supports

2.3 Loading Conditions

As the aim of this research was to model real time traffic loading and its effects on the structure, a scaled trolley (representing a vehicle) was used. A road base was constructed on the backfill, and a flexible track system was built over the road base to enable movement of the model vehicle. The height of the backfill above the extrados of the crown was varied (equivalent to full scale heights of 0.5m, 0.3m and 0.2m). The

lower the level of backfill the less dispersal of load occurs creating a more onerous loading effect on the arch ring. The mass of the vehicle was changed by stalking dead weights on the trolley. The track was marked at intervals of 0.08m along the entire span of the roadway. A complete loading cycle involved moving the vehicle from left to right (1.2m travel) and return to original place. The readings were taken when the model vehicle come to halt at a pre-selected location on the track. A typical test involved three runs on the track; including forward and return travel.

3 STABILITY TEST AND MONITORING

3.1 Test procedure

A previous stability test on a 5m span by 2m rise arch ring, Taylor et al. (2006) showed the arch was stable during backfilling. However due to the use of light weight PVC voussoirs in this investigation, the arch could be less stable and experience greater uplift at the crown during backfilling operations. To ensure the stability of the arch ring it was carefully monitored. The backfilling operation was carried out by placing ~ 0.05m deep layers of the well-graded backfill material to each side of the arch. The distribution of load equally to either side of the arch ring was aimed at minimising the effects of asymmetric loading. Readings for all of the sensors were taken at each increment height of backfill.

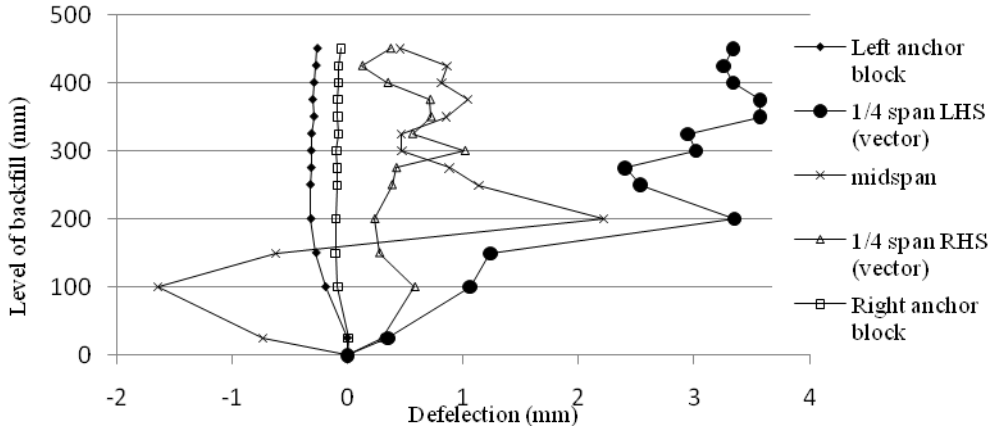

Figure 3: Arch deflections during backfilling operations.

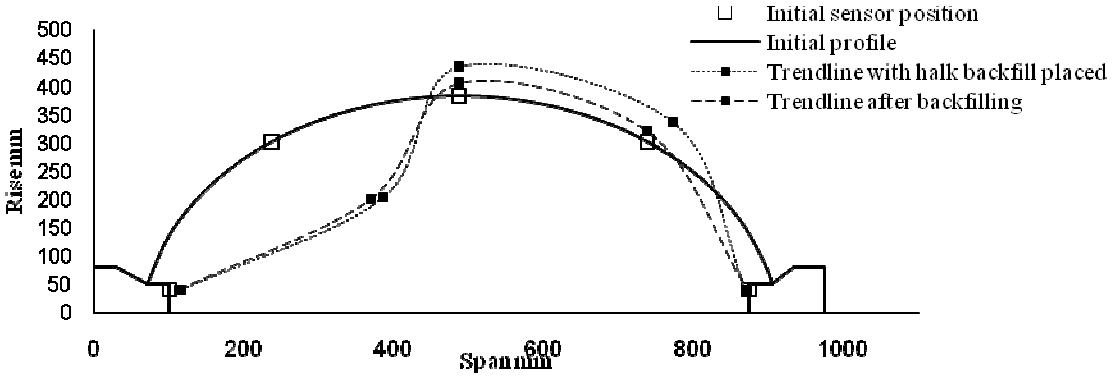

Figure 4: Exaggerated (x50) deflections of the arch after backfill.

3.2 Results from the monitoring of backfilling

The readings show a non-symmetric response to the backfilling operation and this could have been due to the direction of loading causing sway in the whole arch ring. A summary of the deflections at various times throughout the backfill operation is given in Figure 3. Figure 4 shows the exaggerated (x 50) deflected shape of the arch ring when the backfill level was just above the crown of the arch and also after backfilling. The maximum movement in the crown was 1.04mm upwards, this occurred when the granular backfill was at the height of the crown of the arch. This was due to the lateral pressure of granular backfill creating an inwards movement at the sides of the arch and subsequent upwards movement at the crown. Subsequent load on top of the crown had a beneficial effect on the deflection. The maximum movement at the sides of the arch occurred in the transducers on the LHS at the third span. At the end of the backfill operation, the maximum inwards movement was 3.5mm at the third span. The results of the monitoring showed that the arch was sufficiently stable during backfill operations.

4 MONITORING RESULTS

When the load was at a maximum of 250kg (equivalent to a full scale partial axle load of 300KN for bridge structure) and the backfill at the minimum level of 50mm above the crown extrados, there was no visible signs hinge formation. For masonry arch failure, a hinge mechanism would generally occur. However the bearing capacity of the road and backfill was exceeded which prevented any further increase in loading.

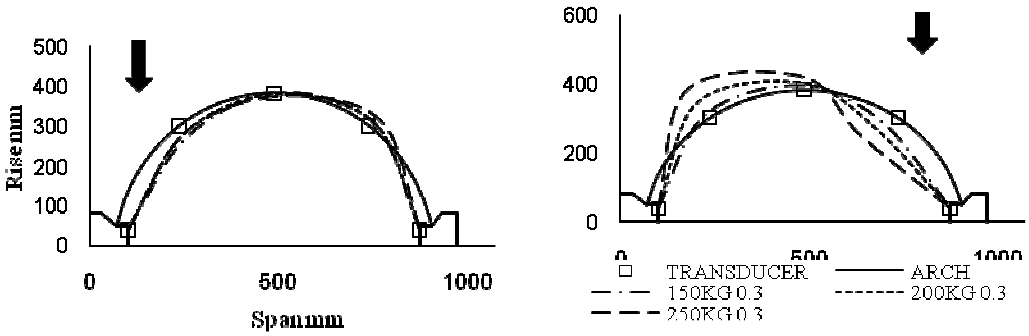

Figure 5: Exaggerated deflections of the arch during loading.

4.1 Deflections

The deflections of the arch ring increased with increasing axle load and the largest deflections occurred when the load was applied over the third span, where a hinge could occur. Figure 5 shows the data for the axle load at the third span and the inward movement of the arch ring below the load and outward movement of the ring on the opposite side. The initial loading for each test was from left side and the results show that this caused permanent deformations in the arch ring. Therefore for all three tests there are greater deflections on the left side (Figure 5).

For the majority of tests the greatest deflection was encountered on the third run. In general when a load of 250kg was applied the deflections increased by about 15% between the first run and the third run. In some cases the recovery of the H2/V2 deflections was as little as 53% which is not within the acceptable limits. The results show that the structure exceeded its elastic limit and permanent deformations occurred.

4.2 Strain results

The distribution of vertical load in the support beam (Figure 2) was not constant as shown by the ERS results in Figure 6; the ERS2 recorded a greater strain, which corresponded with the higher deflections when the load was directly above the right side of the arch ring. This could have been caused by a longitudinal surcharge through the backfill from the axle as it travelled across the pavement. Both ERS show a similar behaviour but Figure 6 shows that ERS2 had higher strain due to higher pressure. The results for varying the load showed that the greatest combined load occurred when the load is at the centre of the arch, corresponding to the location with the least amount of backfill. Figure 6 also shows that as predicted the vertical load transferred to the beam increased as the level of backfill decreased.

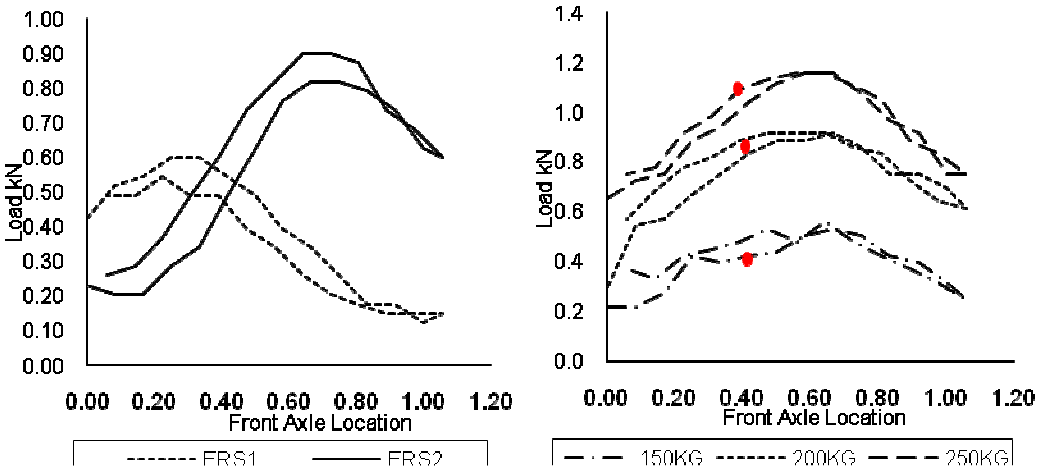

Figure 6: Distribution of Vertical load between ERS strain monitors and combined vertical load on ERS strain monitors for varying load.

4.3 Pressure Sensor results in the arch ring

Pressure sensors (PC1-5) were installed into five of the voussoirs (as Figure 2). The pressure sensors were installed in order to gain a clearer understanding of the soil/structure interaction. The results from the pressure sensors were not as consistent as the other sensors. In most cases such sensors are subjected to a constant pressure, during this testing a variation in pressure across the surface occurred due to change in the arching thrust between and through the voissoir. The granular backfill acted to disperse the axle load but may have created concentrated loading points on the sensors. The arch was also free to deflect inwards creating a negative drop in pressure at the interface. Ideally, the pressure sensors should have been contained wholly within the backfill or voussoir. Further testing of these sensors in granular materials will give more information on the correct means of application for monitoring of soil/structure interaction. At PC1, under the maximum load and lowest level of backfill above the crown, the pressure was higher under forward movement in comparison to the load travelling in reverse. This indicated that the dispersal of load spread was more concentrated in the direction of travel as shown in Figure 7.

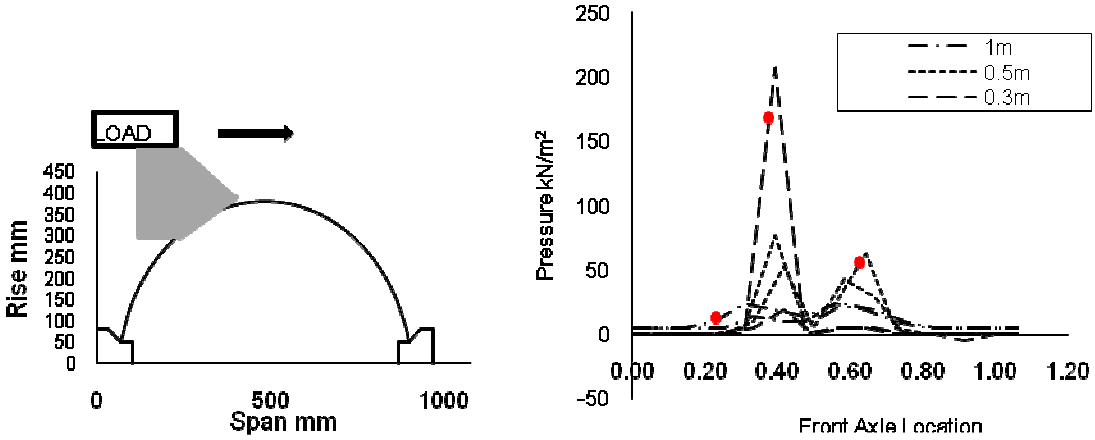

Figure 7: Load spread in forward movement and pressure Cell 3 results varying backfill level with a constant load of 250kg.

The results of PC3 in Figure 7 show that highest pressure occurred with the lowest level of backfill that is 0.3m above the extrados crown. A pressure of 206kN/m^2 was measured when the front axle was over the midspan location under reverse movement; this is close to the bearing capacity of the unconstrained soil. Figure 7 shows the differences in pressure under forward and reverse movement and is consistent with the results for this PC3. The results also showed a significant difference between run 1 and run 2 of the same test, and this may have been due to permanent damage caused to the road base after the first run. This could also explain the difference in pressures under run 1 to run 2. The additional peak in the reverse run occurs when the back axle was close to the midspan. The axle on the track acted as a series of point loads, and movement of the track probably changed the dispersal of loading through the backfill. Another possible explanation for the change in dispersal of load was the differences in pulling and pushing the vehicle. It was much easier to pull and was faster but with more dynamic amplitude compared to pushing.

4.4 Vibrating Wire strain gauge (VWSG) results

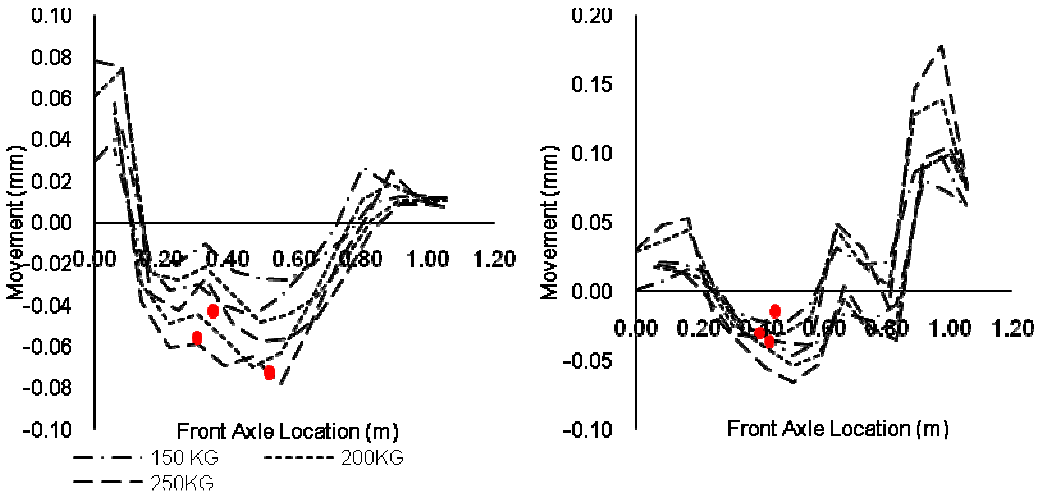

Figure 8: Results for VW gauges 1 and 2 for varying load with a constant backfill level of 0.3m.

VWSG were used to measure joint openings between the voussoirs. The results VWSG were consistent with the transducer results. The strain measured by the sensors was converted to a joint opening as all of the tensile strain was due to the joint opening. Similarly to previous results the reverse movement had a more significant effect on the openings as shown in Figure 8, as the axle load increase the joint openings increased. As the axle load was applied VW1 measured tension but when the load is moved over, towards the location of the VW1 the arching thrust caused compression at this position. This is similar to the findings in the deflection results where H2/V2 had a maximum outward movement. Sensor VW2 showed a similar of the pattern to that of VW1; but with slight difference due to the asymmetric dispersal pattern under forwards and reverse movements. Additionally in VW2, there was a shift in tensile strains at the same time as a shift in compression strains at the opposite third span, showing that these were the most likely positions for a hinge to form. The maximum tension strain or joint opening occurred at VWG2 and was almost double that of VWG1; this corresponds with previous findings that the right side of the arch was stiffer therefore allowing less movement in that direction, the greater movement in the left direction allows for greater hinge opening at the location of VWG2. The large peak in compressive stress on VWG2 at 0.6m only occurred when the backfill level was reduced to 0.3m, and there was no peak in tensile strain in VWG1 at higher backfill levels. A much smaller peak in compressive strain in VWG2 did occur at the same location for the 0.5m backfill which also corresponds to a small peak in tensile stress in VWG1. This shows that as there would be hinge opening on one side this would cause compression on the opposite side

5 NON LINEAR FINITE ELEMENT ANALYSIS (NLFEA)

5.1 Finite Element Model

The finite element model was created using the commercial package ABAQUS and various nonlinear material properties were adapted to model the behaviour of the arch. A Concrete Damaged Plasticity model was adopted for the arch ring. The material for the arch ring is defined as one with high compressive strength and little or no tensile strength. The granular backfill is modelled using a Drucker-Prager plasticity model. The Drucker-Prager material law requires three material parameters the internal angle of friction Ø, cohesion c, and the dilation angle of the backfill material, Audenaert et al. (2008). The material properties were obtained from the backfill used in the laboratory model study. The angle of friction and angle of dilation are taken to be 40^0, Youngs Modulus 50Ma, Poisson's Ratio as 0.2 and the cohesion as 0.015. In reality the backfill which was used was very sandy and therefore would little or no cohesion. However if a value is not entered the analysis is unstable unless side supports are constructed. The load model is created with a Young's Modulus of 2E5 MPa and a Poisson's Ratio of 0.3. The density of the material varied to represent the different loads used in the laboratory testing.

The numerical model has the capability to analyse using implicit or explicit methods. An explicit analysis was used as it allows dynamic analysis and this does not require equilibrium of the externally applied loads and the internal forces at each load increment to continue. This provides a solution to the convergence problem which can occur in a static implicit analysis. Previous studies have shown that, due to the nonlinearity of the backfill and arch ring, the explicit method is more suitable, Robinson et al. (2010), Zheng et al. (2010). The boundary conditions are applied to the model.

Once the boundary conditions have been applied the load is applied in steps. The load is applied in two steps the first being the gravity loading step and the second step is the applied loading.

5.2 Results

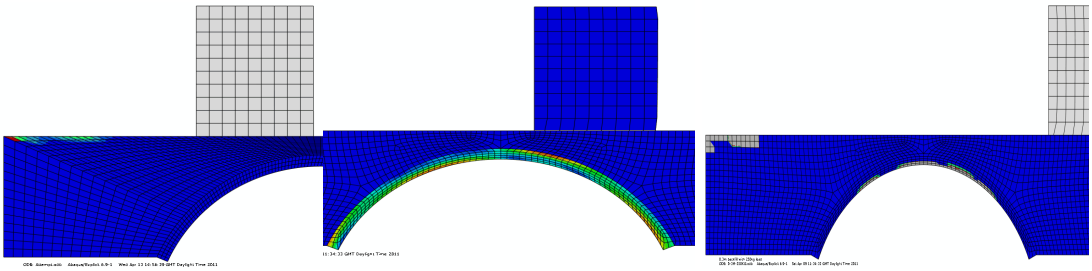

Figure 9: Stresses on backfill material after initial loading, stresses in the arch ring and permanent damage caused to arch ring and backfill by applied load.

The results from the NLFEA give an insight into the behaviour of the material and also model the behaviour of the structure. The model can be used to determine the peak load on the arch and the most critical loading position. The NLFEA is part of ongoing research as the changes in the material properties due to confinement and loading history are not fully established. However the behaviour of the structure under the dynamic loading was analysed and this showed that the location of the initial application of the load had a permanent effect on the structure. Figure 9 shows permanent damage in the soil at the location of the applied load even after the load has moved across the structure and the strain pattern in the NLFEA is similar to that measured by the sensors. The VWSG results showed that when the load was at this location, there was opening in VWG2 and compression in VWG1. Compression in the extrados would cause tension in the intrados. The laboratory model tests show that there was a higher vertical load on the right side of the model; looking at the results in Fig 10 it appears that the results from NLFEA are consistent with this.

6 CONCLUSIONS

The results from the SHM showed the significance of the backfill in contributing significantly to the overall strength and stability of the arch system. The sensors were able to show the effects of a dynamic load and, in particular, the results of longitudinal surcharge causing asymmetric loading on the arch ring. The sensors were also able to validate the NLFEA model. However, the SHM results showed greater deflections on one side of the arch and this was probably due to an overall sway in the system. To examine this further, a parametric study is to be carried out using the NLFEA and varying the geometry to provide asymmetrical response. The NLFEA in this study provided horizontal and vertical reactions at the support locations which showed reasonable agreement with the pressure sensors but further studies are ongoing to investigate the use of pile foundations for the support the structure.

7 REFERENCES

Audenaert, A. Fanning, P. Sobezak, L & Peremans, H. (2008). 2-D analysis of arch bridges using an elasto-plastic material model. Engineering Structures. 30 (3), P845-855.

Fanning P J and Boothby T E, (2001) Three-dimensional modelling and full-scale testing of stone arch bridges, Computers and Structures, v 79, n 29-30, November, 2001, p 2645-2662

Robinson, D., Johnston, R. & Taylor, S. (2010). Finite element analysis of skewed FlexiArch.

Taylor S E, Gupta A, Kirkpatrick J, Long A E, Rankin G I B and Hogg I. (2006) Development of a novel flexible concrete arch system, 11th International Conference on Structural Faults and Repairs, Edinburgh, June 2006.

Taylor S E, Gupta A, Kirkpatrick J, Long A E, Rankin G I B and Hogg I. (2009) Monitoring of Tievenameena Flexiarch Bridge, Proceedings of Advanced Composites in Construction. P342-351. 2009

Zheng, Y. (2010). Non-linear finite element analysis of masonry arch bridges reinforced with FRP. Proceeding of 10th International Arch Bridges Conference .